GRAIN BOUNDARIES AND GRAIN SIZE DISTRIBUTIONS IN NANOCRYSTALLINE DIAMOND FILMS DERIVED FROM FULLERENE PRECURSORS

R. Csencsits[1], C. D. Zuiker[2], D. M. Gruen[2], and A. R. Krauss[2]

[1]Materials Science Division,
Argonne National Laboratory, Argonne, Illinois 60439 USA

[2]Materials Science and Chemistry Divisions
Argonne National Laboratory, Argonne, Illinois 60439 USA

Submitted for the

Proceedings of the International Conference POLYSE '95
"Polycrystalline Semiconductors - Physics, Chemistry and Technology"
Villa Feltrinelli, Gargnano, Italy

September 9-14, 1995

*Work supported by the U.S. Department of Energy, BES-Materials Sciences, under Contract W-31-109-ENG-38.

GRAIN BOUNDARIES AND GRAIN SIZE DISTRIBUTIONS IN NANOCRYSTALLINE DIAMOND FILMS DERIVED FROM FULLERENE PRECURSORS

R. CSENCSITS[1], C. D. ZUIKER[2], D. M. GRUEN[2], AND A. R. KRAUSS[2]

[1]Materials Science Division, Argonne National Laboratory, Argonne, Illinois 60439 USA

[2]Materials Science and Chemistry Divisions, Argonne National Laboratory
Argonne, Illinois 60439 USA

Keywords: diamond, C_{60}, grain boundary, grain size, TEM, fullerenes, nanocrystalline

Abstract. Diamond films produced by traditional CH_4/H_2 methodologies usually display a columnar growth of micron-sized crystallites. Such films have been extensively characterized by a wide variety of techniques, and their microstructures have been studied in detail. By contrast, nanocrystalline diamond films have been much less investigated, perhaps because they are often referred to in the literature as "poor quality" diamond. The recent development of film growth from C_{60}/Ar mixtures may begin to change this situation in that this methodology results in very pure diamond, as demonstrated by the work discussed here and in earlier papers [1-3].

Diamond films grown using C_{60} as a carbon source have been shown to be nanocrystalline with average grain sizes of 15 nm and standard deviations of 13 nm. The measured grain size distribution for two separate films, each based on measurements of over 400 grains, were found to be very similar and were well-approximated by a gamma distribution. Unlike typical CVD grown diamond films, these nanocrystalline films do not exhibit columnar growth. From the measured grain size distributions, it is estimated that 2% of the carbon atoms are located in the grain boundaries. The structure of the carbon in the grain boundaries is not known, but the films survive extended wear tests and hold together when the substrate is removed, indicating that the grains are strongly bound. The grain boundary carbon may give rise to additional features in the Raman spectrum and result in absorption and scattering of light in the films. We also expect that the grain boundary carbon may affect film properties, such as electrical and thermal conductivity.

Introduction

In earlier work [1], we have used high-resolution transmission electron microscopy (HRTEM) to investigate the microstructure of diamond films grown by plasma-assisted chemical vapor deposition using fullerene precursors [2,3]. HRTEM observations of as-grown films revealed an array of larger crystals within a polycrystalline matrix of much smaller crystallites (< 20 nm). The randomly oriented small crystallites were nearly free of structural imperfections such a stacking faults or twins, while the larger ones had preferred <110> orientations with respect to the Si(100) substrate and showed evidence of structural defects on the periphery of the crystals.

The films grown from fullerene precursors have now been found to be extremely smooth with root mean square (rms) surface roughness of 20-40 nm using both laser reflectance interferometry (LRI) and atomic force microscopy (AFM) measurements [4]. The tribological properties of the films have also been investigated [5] and yield wear rates of 1.8×10^{-8} mm^3/N•m after 2.4×10^6 cycles using Si_3N_4 balls with 5N loadings. These results indicate two orders of magnitude improvement over diamond films grown by conventional CH_4/H_2 methodologies, which typically have surface roughness in the micron range due to the micron size crystallites in the deposits.

The superior tribological properties of the fullerene-generated films make it important to understand the cohesive forces and the nature of the carbons, which provide the intergranular bonding between the randomly oriented nanocrystallites. It is certainly arguable that the erosion resistance of the films is due in part to their high-angle/high-energy grain boundaries, which make it very difficult to deform the material. From the earlier HRTEM work (see Fig. 3 in Ref. [1]), it is known that the nanocrystallites are highly stepped, perhaps due to the fact that dislocations are

"gettered" at the grain boundaries. The resulting low strain field and high activation energy for grain diffusion give the material "glass-like" properties.

The lowest free energy configuration for the nanocrystalline diamond is achieved by bond bending and stretching at the grain boundaries. The nature of the resulting carbon-carbon bonds, the sp^2/sp^3 ratio, for example, as well as the stability of nanocrystalline diamond relative to nanocrystalline graphite is being studied theoretically [6].

The present work was undertaken to learn more about grain size distributions and the fraction of carbon residing at the grain boundaries so as to provide accurate information as input to the theoretical models of this fascinating new material.

Film Preparation

Diamond films were deposited in a microwave plasma chemical vapor deposition reactor (ASTeX PDS-17) as previously described [2,3]. The films were grown on single-crystal silicon wafers polished with 0.1 μm diamond particles to enhance nucleation density. Film growth was monitored in situ using laser reflectance interferometry to determine growth rate and stop growth at the desired thickness. The films were grown with 2 sccm H_2, 98 sccm Ar and C_{60} vapor, 100 Torr pressure, 1500 W of microwave power, and a substrate temperature of 850 °C. A quartz transpirator is used to introduce C_{60} into the reactor. Fullerene-rich soot, consisting of approximately 10% C_{60}, was purchased from the MER Corporation and placed in the transpirator. The soot was heated to 200 °C under vacuum for two hours to remove residual gases and hydrocarbons. The tube furnace and transport tube were heated to between 550 and 600 °C during operation to sublime C_{60} into the gas phase. Argon gas was passed through the transpirator to carry the C_{60} vapor into the plasma.

Microstructure

The microstructure of the diamond films grown from fullerene precursors in an argon plasma was studied using transmission electron microscopy (TEM). To observe and measure the diamond grain size distribution, plan-view TEM specimens were prepared. In order to observe the grain size and shape along the direction of film growth, cross-section TEM specimens were prepared. Images and electron diffraction patterns were recorded in the Philips CM30 TEM operated at 300 kV and in the high-resolution JEOL 4000EXII TEM operated at 400 kV (point-to-point resolution is 0.17 nm).

Preparing TEM specimens is as much art as science. Throughout the last decade several symposia have been devoted to the subject [7-9]. Some details of our procedures are outlined here. To prepare plan-view TEM specimens, a 3 mm square piece of the sample was cleaved, and a 3 mm round, slotted copper grid was glued to the diamond film side using M-bond 610 epoxy. The copper grid facilitates the handling of the TEM specimen. The silicon substrate was mechanically thinned to 50 μm. The center of the specimen was further ground and polished to less than 10 μm using a VCR dimpler. With the diamond side protected from redeposition with a glass slide, the specimen was ion milled from the silicon side until perforation with 6 kV nitrogen ions. The resulting specimen had a hole in the center of the electron transparent diamond film that could be imaged in the TEM. In the areas observed in the TEM, only diamond film was present; all of the silicon substrate had been removed.

To prepare cross-section TEM specimens, two (3 mm × 8 mm) pieces of the sample were cleaved and glued face-to-face with M-bond 610 epoxy. Two pieces of silicon were glued to the backs of the sample pieces producing a four-layer sandwich that was held in a vise and cured in a vacuum oven at 110 °C for four hours. A 1.5 mm thick slice of the sandwich was made using a slow speed diamond saw. One side of the cross-section specimen was polished with diamond lapping films of progressively finer grit size until a mirror finish was obtained. A slotted copper grid was glued to the polished side using M-bond 610 epoxy. After curing, the specimen was turned over and ground down to 120 μm total thickness. Then the specimen was dimpled and polished to less than 10 μm. The specimen was finally ion milled from both sides until perforation with 6 kV nitrogen ions.

Figure 1 is a bright field plan-view TEM image showing the grain size distribution typical for the diamond films grown from fullerene precursors. Shown as an inset in Fig. 1 is the selected area electron diffraction (SAED) pattern formed from a 7 μm^2 area of the film. The continuous sharp rings indicate randomly oriented grains, and their spacings correspond to carbon in the diamond

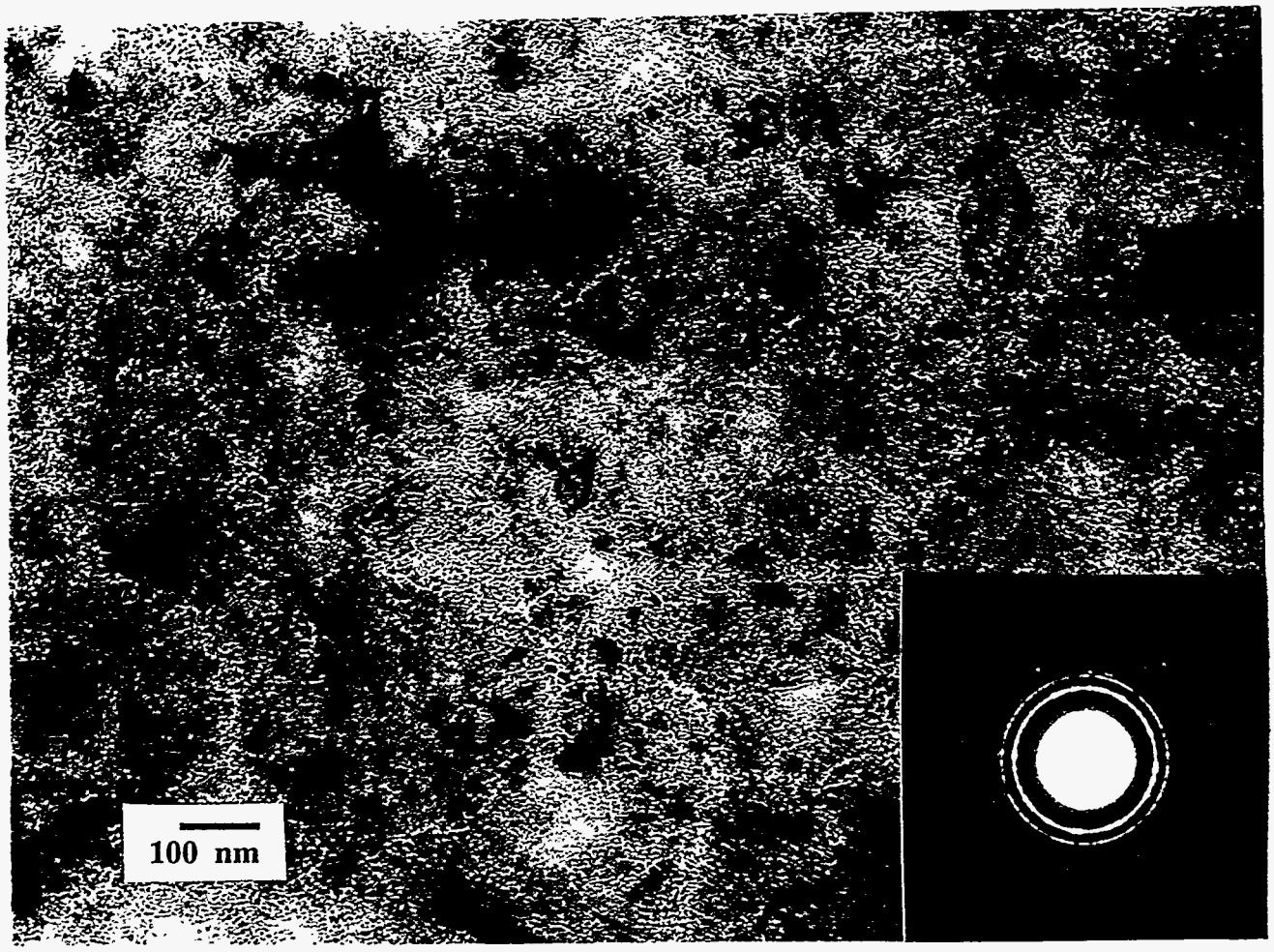

Fig. 1. Plan-view bright field TEM image showing the grain size distribution in diamond films grown from fullerene precursors. The electron diffraction pattern is inset and shows the random orientation distribution of the diamond grains.

cubic form. In a bright-field TEM image, only those grains in favorable orientations (diffraction conditions) appear dark with distinct boundaries. Grain size measurements from bright field images inherently count only those grains that are diffracting, such that they are dark in the image. This is not generally a problem so long as the grains are equiaxed.

The "white lines" observed in Fig. 1 are an interesting feature observed in all diamond film samples grown from fullerene precursors. Some lines are faint and thin, while others appear thicker and more distinct. The white lines undergo bright and dark contrast reversals when changing from an underfocused to an overfocused objective lens condition. They also undergo contrast reversal as the sample thickness changes. These TEM image contrast changes are consistent with a lower electron scattering potential in these regions of the sample. However, when observing these specimens at very high magnification and in high-resolution imaging conditions, no voids or cracks have been observed. Also, these samples do not crack or fall apart along these lines even when the sample is 10 nm to 30 nm thick.

Consistent with these observations is the interpretation that the white lines represent grain boundaries. TEM images are two-dimensional projections of the through-thickness scattering of the specimen. The diamond specimens have the thickness of several grains, and therefore overlapping grains and grain boundaries are observed in the image. In regions where grain boundaries stack upon one another, the white lines are wide and distinct in the image. In other regions where the grain boundaries are not aligned, the white lines are fine and only clearly visible at high magnification. Verification of this interpretation is the subject of future work.

A typical cross-section TEM image of a diamond film is shown in Fig. 2 with its corresponding electron diffraction pattern. One can observe in this image that the diamond grains grown from fullerenes are not columnar and are generally equiaxed. The inset SAED pattern consists of the

single-crystal silicon [110] pattern and three rings (111, 220, 311) of the polycrystalline diamond pattern. This indicates once again that the deposited diamond film consists of randomly oriented grains. It is clear from this cross-section image that there is continuous nucleation and growth of diamond grains throughout the thickness of the deposited film.

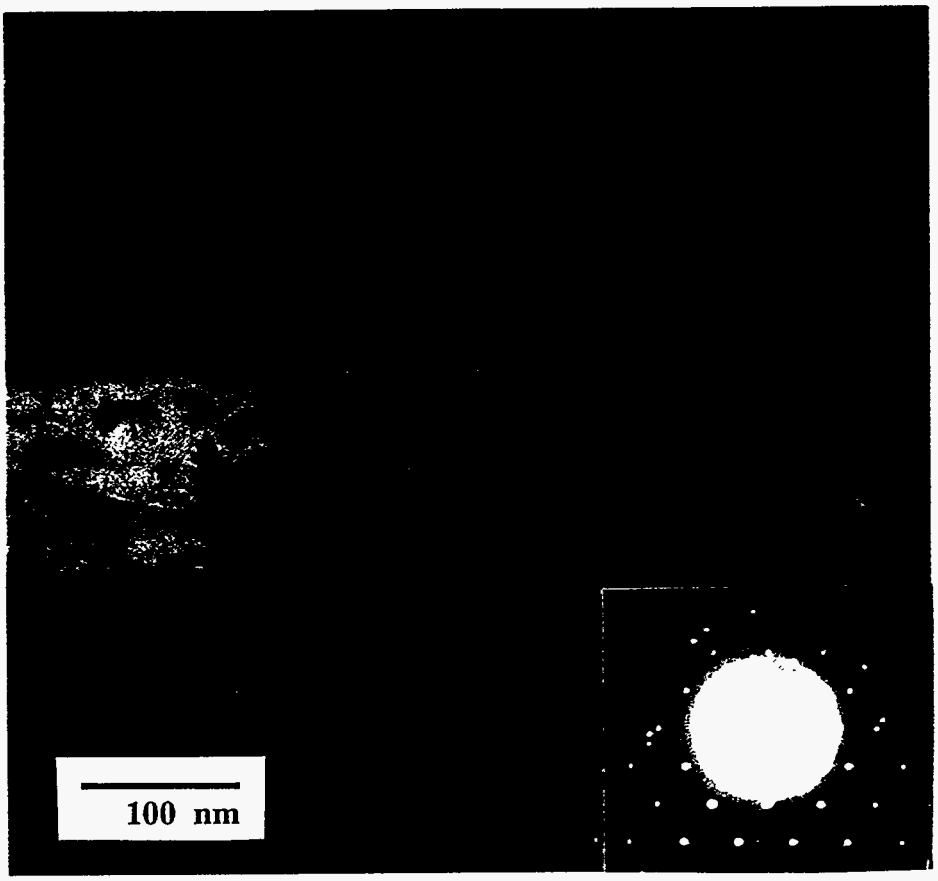

Fig. 2. Cross-section TEM image and SAED pattern of diamond film grown on silicon substrate.

After observation of many plan-view bright-field and dark-field TEM images and their corresponding diffraction patterns, as well as cross-section TEM images, we conclude that diamond films grown from fullerene precursors consist of randomly oriented grains, and that grain size measurements from bright-field TEM images are therefore statistically meaningful.

Due to the small size of the grains and the dependence of grain visibility on diffraction condition in bright-field TEM images mentioned above, the ASTM E112-85 standard grain size measurement procedures could not be used [10]. Instead, the following method was used for determination of the diamond grain sizes. Grain sizes were measured from enlarged prints of TEM images like the one shown in Fig. 1. The magnification of the print was 63,000 times. All discernible grains wholly or partially contained within a rectangular area $140 \times 3800\ \mu m^2$ were measured. The rectangular area was chosen to include a specimen thickness gradient; therefore, both thinner and thicker regions of the diamond film were measured. For the sample shown in Fig. 1, some 467 grains were measured. The minimum and maximum grain sizes are 3.2 nm and 103 nm, respectively. The median grain size is 12.7 nm, while the average grain size is 14.9 nm with a standard deviation of 12.9 nm. These statistics are shown graphically in Fig. 3.

Figure 4 is a high-resolution TEM image of several diamond grains showing the 0.206 nm fringes that correspond to the (111) diamond lattice planes. In regions where a grain is oriented with the [110] direction parallel to the electron beam direction, two sets of (111) planes are imaged as cross fringes. In most regions, the grains are not aligned so fortuitously, and only one set of (111) planes are imaged as fringes. A relatively distinct grain boundary can be observed around a 20 nm × 35 nm grain in the center of the image. The width of this grain boundary appears to be between one-to-two lattice spacings wide. From observations of this type, we estimate the width of the grain boundaries in these films to be 0.25 nm to 0.40 nm.

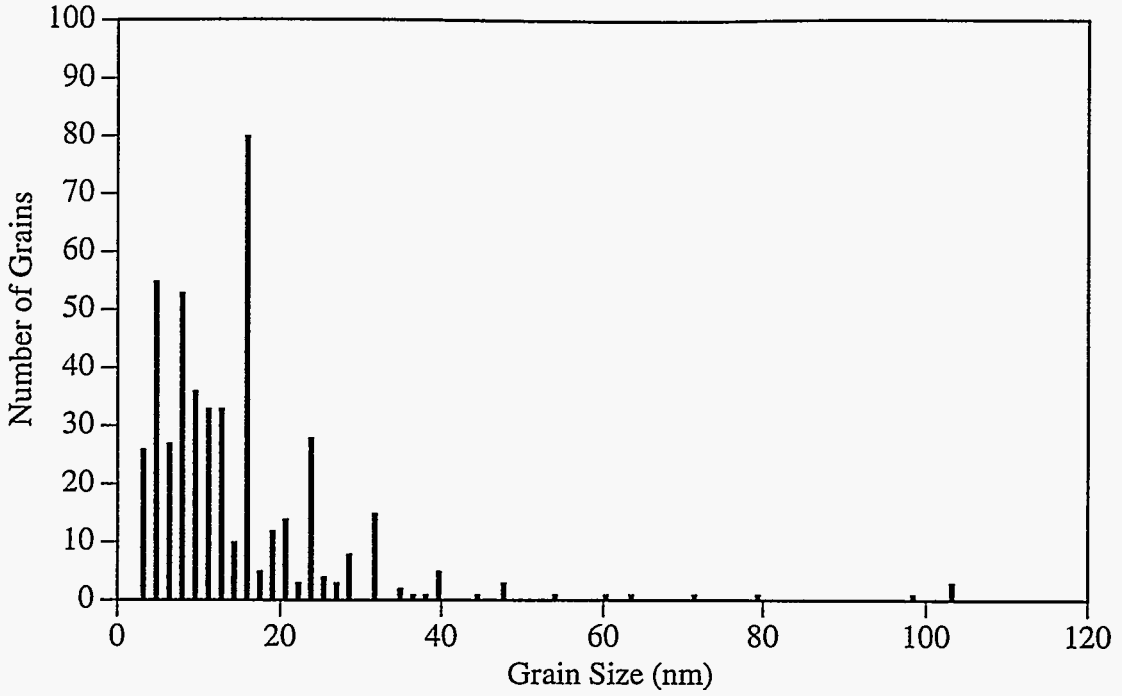

Fig. 3. Plot of diamond grain size distribution measured from bright-field TEM images.

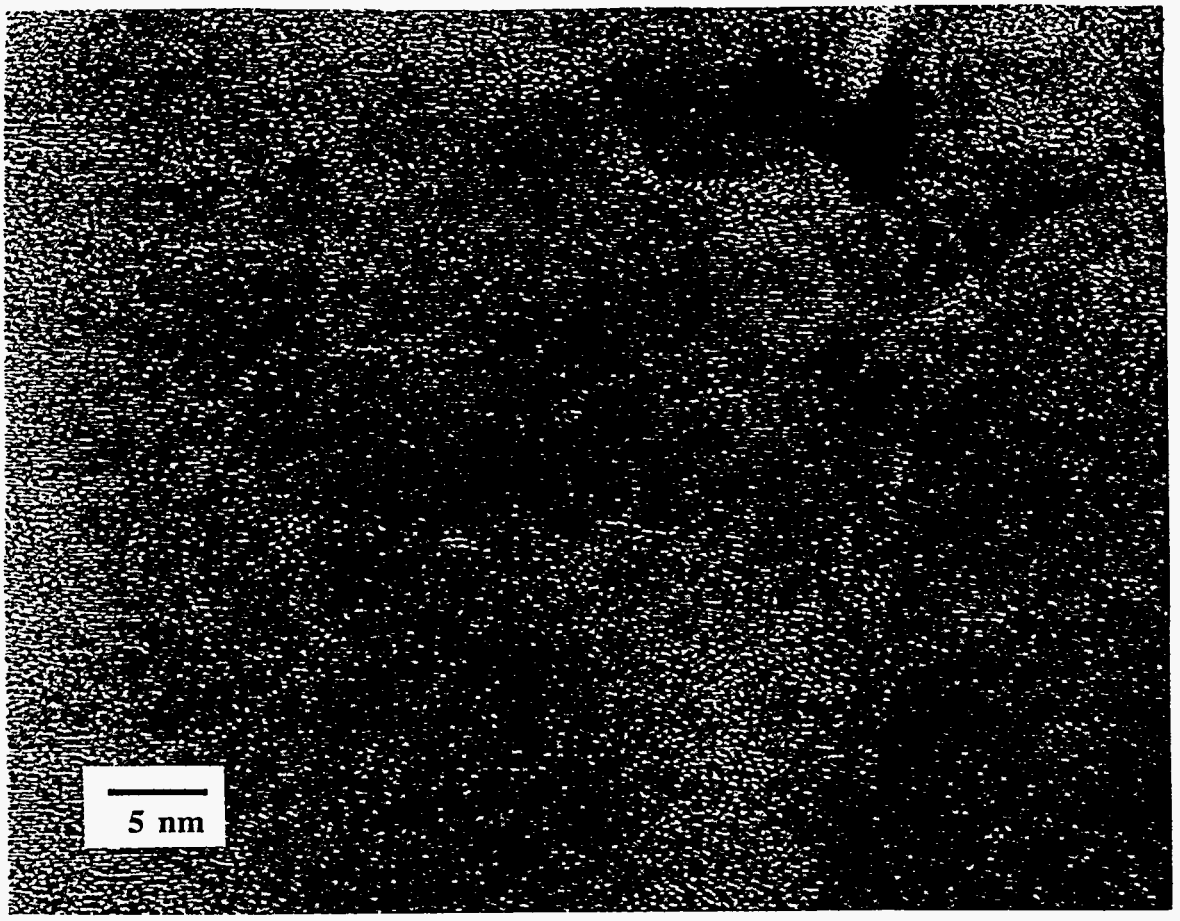

Fig. 4. HRTEM image showing several diamond grains and grain boundaries.

Fraction of Carbon Atoms at Grain Boundary

The fraction of atoms residing at the grain boundaries in a film is expected to have a significant effect on many properties of diamond films. For example, grain boundary atoms may give rise to additional features in the Raman spectrum, may lead to absorption and scattering of light by the film, and from the point of view of the present paper, may have a substantial influence on tribological properties. The fraction of atoms that are located at grain boundaries depends on both the grain size distribution and the thickness of the grain boundaries within the film. Both of these characteristics have been measured for the C_{60} grown films, as described above, allowing calculation of the fraction of atoms that reside at the grain boundaries.

The fraction of atoms located in the grain boundary of the film can be calculated using the following expression:

$$\text{grain boundary fraction} = \frac{N\int_0^\infty f(x)\eta(x,d)\rho_{gb}x^3dx}{N\int_0^\infty f(x)\left[(1-\eta(x,d)\rho_d)+\eta(x,d)\rho_{gb}\right]x^3dx}. \quad (1)$$

In Eq. (1), N is the total number of grains in the film, x is the grain size, f(x) is the probability density function, pdf, for the grain size distribution, $\eta(x,d)$ is the volume fraction of the grain boundaries of width d in a grain of size x, ρ_{gb} is the atom number density of the grain boundary, ρ_d is the atom number density of diamond, and x^3 is the volume of the grain. The product f(x)dx is the fraction of grains with sizes between x and x + dx. The numerator is the total number of atoms in the grain boundaries of the film, while the denominator is the total number of atoms in the film. The ratio is the fraction of atoms in the grain boundaries of the film. For simplicity, the grains are assumed to be cubes leading to the following expression for $\eta(x,d)$:

$$\eta(x,d) = 1-\left(\frac{x-d}{x}\right)^3, \quad x \geq d;$$
$$= 1, \quad x < d. \quad (2)$$

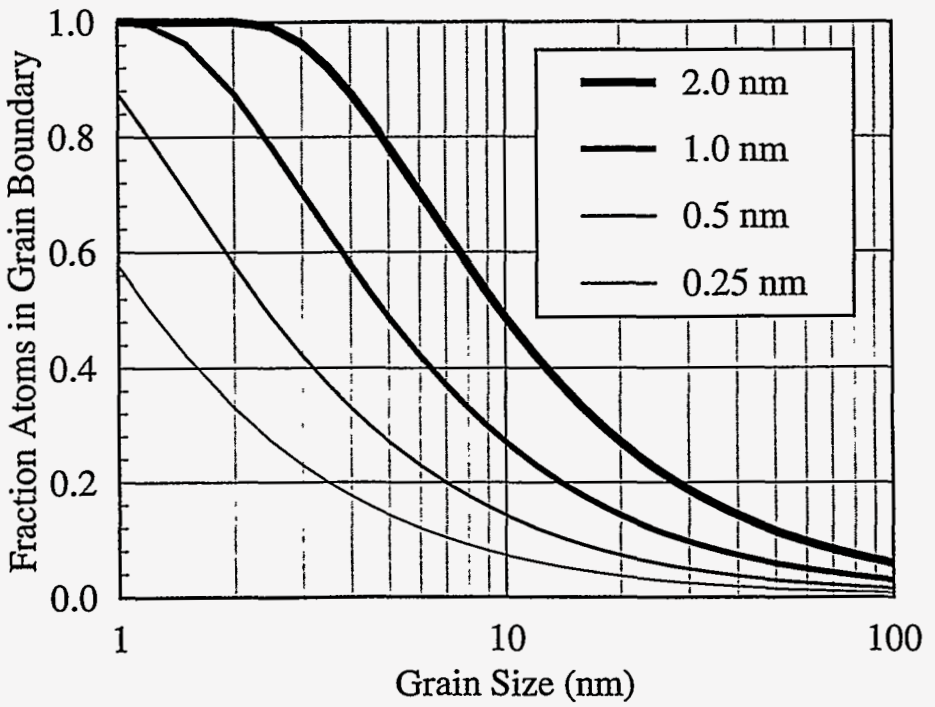

Fig. 5. Fraction of atoms at grain boundaries as a function of grain size for grain boundary widths of 0.25, 0.5, 1, and 2 nm.

Plots of $\eta(x,d)$ as a function of grain size, x, are shown in Fig. 5 for grain boundary widths, d, of 0.25, 0.5, 1, and 2 nm. For diamond films, 0.25 nm represents a grain boundary width of approximately two atoms. From Fig. 5, it is clear that for the C_{60} grown diamond films with grain sizes of around 10 nm, a significant fraction of the atoms are located at the grain boundaries. From the HRTEM images, d was determined to be between 0.25 and 0.4 nm, while grains were typically 10-20 nm in size. Since $x >> d$, $\eta \approx d/x$ in Eq. (2). Assuming $\rho_{gb} = \rho_d$, Eq. (1) reduces to the following simple expression:

$$\text{grain boundary fraction} = \frac{3d\langle x^2 \rangle}{\langle x^3 \rangle}. \tag{3}$$

In Eq. (3), the quantities in brackets denote expected values. The factor of 3 arises from the assumption that the grains are cubes and would be a factor of 1.5 if spherical grains were assumed. For film 941005b, $\langle x^2 \rangle = 389.5$ nm^2, $\langle x^3 \rangle = 18472$ nm^3, and $0.25 \text{ nm} < d < 0.40$ nm. From Eq. (3), the fraction of atoms at the grain boundaries is in the range 0.016 to 0.025. Since diamond has the highest atom density of any known material, the atom density in the grain boundaries must be lower than that in the grains, and Eq. (3) overestimates the grain boundary fraction. Uncertainty in the shape of the grains and grain boundary width also increases the uncertainty in this calculation. Thus, the calculated grain boundary fraction is only considered accurate to within a factor of 2 or 3.

The measured grain size distribution for film 941005b is based on measurements of 467 grains. Due to the x^2 and x^3 factors in Eq. (3), large grains are more heavily weighted than small grains, making the calculation sensitive to the small number of larger grains measured. For comparison, the measured grain size distribution for film 940927, which is based on measurements of 440 grains, was also used to calculate the grain boundary fraction. For film 940927, $\langle x^2 \rangle = 430.2$ nm^2, $\langle x^3 \rangle = 20949$ nm^3, and $0.25 \text{ nm} < d < 0.40$ nm. From Eq.(3), the fraction of atoms at the grain boundaries is in the range 0.015 to 0.025. The distributions for the two films lead to almost identical atom fractions at the grain boundaries. This indicates that the grain size distribution is reproducible and adequately represented by the measurement of around 450 grains.

The measured distributions were compared with various statistical distributions and found to be well approximated by a gamma distribution [11]. The pdf for a gamma distribution is

$$f(x,\alpha,\beta) = \frac{x^{\alpha-1}}{\beta^{\alpha}\Gamma(\alpha)} e^{-x/\beta}, \tag{4}$$

where the mean is $\alpha\beta$ and the variance is $\alpha\beta^2$. The parameters α and β were chosen to match the mean and variance of the gamma distribution to those of the measured distribution. Both distributions are shown in Fig. 6 for film 940927 and show general agreement. The matched gamma distributions for films 941005b and 940927 have $\langle x^3 \rangle$ values of 14545 and 17745 nm^3, respectively. The measured distributions have larger values of $\langle x^3 \rangle$ due to more grains in the tail of the distributions. The lower value of $\langle x^3 \rangle$ for the matched gamma distributions results in a 20-25% increase in the fraction of atoms in the grain boundaries using Eq. (3), which is within the error of the calculation. Thus, the measured grain size distribution can be well approximated by a simple, standard probability function, which results in a similar fraction of atoms in the grain boundaries.

The carbon atoms in the grain boundaries are difficult to study, and the structure is not known. Some information can be obtained from macroscopic observations of the films. First, the grains are strongly bound together. Ball-on-disk sliding tests performed on these films have shown that they exhibit low friction and little wear [5]. If the grains were not strongly bound together, one would expect the films to disintegrate during wear tests. The silicon substrate can be removed from sections of 2 μm-thick diamond films to form 1 cm diameter diamond windows. Since the 2 μm-thick film holds together, the grains must be strongly bound. The films are transparent and appear to be brown in color. This is evidence of absorption within the film, which may be due to the grain boundary carbon atoms. The grain boundaries are expected to scatter phonons and thus reduce the thermal conductivity of these films relative to natural diamond. Finally, the grain boundaries may provide paths for electrical conduction through the films, reducing the resistivity relative to bulk diamond.

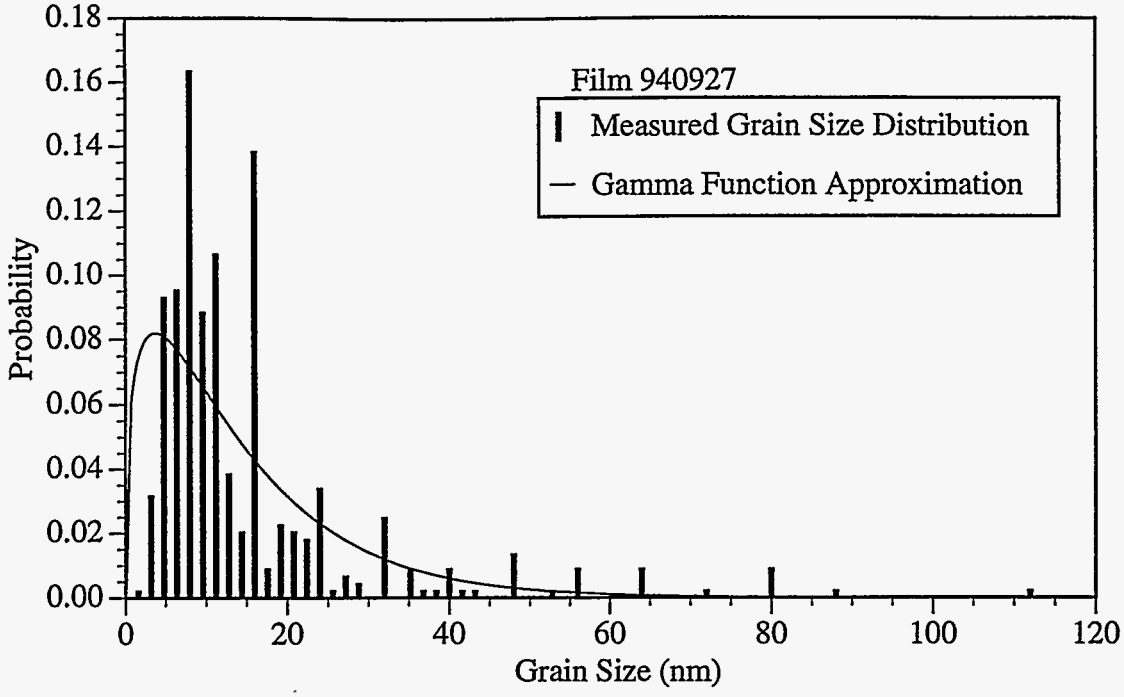

Fig. 6. Comparison of measured grain size distribution and gamma distribution with matching mean and standard deviation.

Conclusions

Diamond films grown using C_{60} as a carbon source have been shown to be nanocrystalline with average grain sizes of 15 nm and standard deviations of 13 nm. The measured grain size distribution for two separate films, each based on measurements of over 400 grains, were found to be very similar and were well-approximated by a gamma distribution. Unlike typical CVD grown diamond films, these nanocrystalline films do not exhibit columnar growth. From the measured grain size distributions, it is estimated that 2% of the carbon atoms are located in the grain boundaries. The structure of the carbon in the grain boundaries is not known, but the films survive extended wear tests and hold together when the substrate is removed, indicating that the grains are strongly bound. The grain boundary carbon may give rise to additional features in the Raman spectrum and result in absorption and scattering of light in the films. We also expect that the grain boundary carbon may affect film properties, such as electrical and thermal conductivity.

Acknowledgements

Work supported by the U. S. Department of Energy, BES-Materials Sciences, under Contract W-31-109-ENG-38.

References

[1] J. S. Luo, D. M. Gruen, A. R. Krauss, X. Z. Pan, and S. Z. Liu, "High Resolution Transmission Electron Microscopy Study of Diamond Films Grown from Fullerene Precursors," submitted for the Proceedings of the Symposium on The Fullerenes: Chemistry, Physics, and New Directions, 187th Meeting of the Electrochemical Society, Reno, Nevada, May 21-26, 1995 (in press).

[2] D. M. Gruen, S. Liu, A. R. Krauss, and X. Pan, J. Appl. Phys **75**(3), 1758-1763 (1994).

[3] D. M. Gruen, S. Liu, A. R. Krauss, J. Luo, and X. Pan, Appl. Phys. Lett. **64**(12) 1502-1504 (1994).

[4] C. D. Zuiker, D. M. Gruen, and A. R. Krauss, MRS Bulletin **XX**(5), 29-31 (1995).

[5] C. D. Zuiker, A. R. Krauss, D. M. Gruen, X. Pan, J. C. Li, R. Csencsits, A. Erdemir, C. Bindal, and G. Fenske, "Physical and Tribological Properties of Diamond Films Grown in Argon-Carbon Plasmas," submitted for the Proceedings of the 1995 International Conference on Metallurgical Coatings and Thin Films Symposium on the Synthesis and Characterization of Diamond and Related Materials, San Diego, California, April 24-28, 1995 (in press).

[6] D. Wolf and S. Phillpot, private communication.

[7] *Specimen Preparation for Transmission Electron Microscopy of Materials*, ed. by J. C. Bravman, R. M. Anderson, and M. L. McDonald, Materials Research Society Symposium Proceedings Vol. 115 (1988).

[8] *Specimen Preparation for Transmission Electron Microscopy of Materials II*, ed. by R. M. Anderson, Materials Research Society Symposium Proceedings Vol. 199 (1990).

[9] *Specimen Preparation for Transmission Electron Microscopy of Materials II*, ed. by R. M. Anderson, B. Tracy, and J. C. Bravman, Materials Research Society Symposium Proceedings Vol. 254 (1992).

[10] *1986 Annual Book of ASTM Standards, Section 3 Metals Test Methods and Analytical Procedures,* Vol. 3.03 Metallography; Nondestructive Testing (ASTM, USA, 1986), p. 115.

[11] R. V. Hogg and E. A. Tanis in *Probability and Statistical Inference*, 2nd edition, Macmillan Publishing Company Inc., New York, 1983.